Optimal Finite Impulse Response Filter Design

Nima Leclerc (nleclerc@seas.upenn.edu)
ESE 531 (Digital Signal Processing)
School of Engineering and Applied Science
University of Pennsylvania

April 7, 2021

Abstract

This work considers the filter design of Finite Impulse Response (FIR) filters applied to audio and image signals and Filter banks. For filter design, both heuristic and systematic methods are used including truncation and optimal order design. A 4-band octave filter bank is also implemented and applied to one-dimensional signals in time.

1 Three Ways of Designing FIR Filters

1.1 Design with Truncation

Here, we implement FIR filtering via truncation. Consider an ideal low-pass filter in the frequency domain shown in Eqt. (1).

$$H_{id}(e^{j\omega}) = \begin{cases} 1, |\omega| \leq \omega_c \\ 0, \omega_c < \omega \leq \pi \end{cases} \tag{1}$$

This ideals how pass filter has an impulse response given by Eqt. (2).

$$h_{ideal}[n] = \frac{\omega_c}{\pi}\text{sinc}(\frac{\omega_c n}{\pi}), -\infty < n < \infty \tag{2}$$

We now implement the filter design for two sizes, $N = 21$ and $N = 101$. To ensure that the system is causal, we must truncate the signal by setting $M = 10$ and $M = 50$. This has the same effect of applying a Boxcar window operation to the impulse response. We then obtained the frequency response in the standard way by taking the Fourier transform of the impulse response. The magnitude of the frequency response $|H(\omega)|$ for $N = 21$ and $N = 101$ are plotted in Figure 1 (both in dB and normal scale). Figures 1(a) and 1(b) show the frequency response in linear scale for $N = 21$ and $N = 101$, while the corresponding plots are shown in log scale in Figures 1(c) and 1(d). First comparing Figures 1(a) and 1(b), we notice that the frequency of the passband ripple for $N = 21$ is considerably smaller than

the corresponding ripple for $N = 101$. Moreover, the $N = 101$ filter experiences a very sharp transition between the passband and stopand region, in contrast to $N = 21$. Finally, the stopband ripple amplitude for $N = 21$ is close to one order of magnitude larger than the case of $N = 21$. The effect of the filter size on the stopband becomes more obvious when comparing the filters in log scale (Figures (1) and (d)). The stopband amplitude drops off more rapidly for $N = 101$, while the $N = 21$ filter's stopband amplitude remains near -20 dB. Collectively, this makes the $N = 101$ filter the ideal design among the two as it has a very sharp pass-stop band transition and small stopband amplitude; however, the benefits of this design are offset by the fact that its order is high, which will contribute to a computationally expensive implementation.

Next, each truncated filter corresponding to sizes $N = 21$ and $N = 101$ is applied to a noisy speech signal by convolving the signal $x[n]$ with the impulse response of each filter $h[n]$. Applying the $N = 21$ filter removes some of the high-frequency noise of the signal, while applying the $N = 101$ filter removes most of the high-frequency noise. Since the dominant noise components are seen at high-frequencies, both low-pass designs were effective at filtering out most of the noise from the signal. The code use to perform the truncation of these filters is attached in the Appendix.

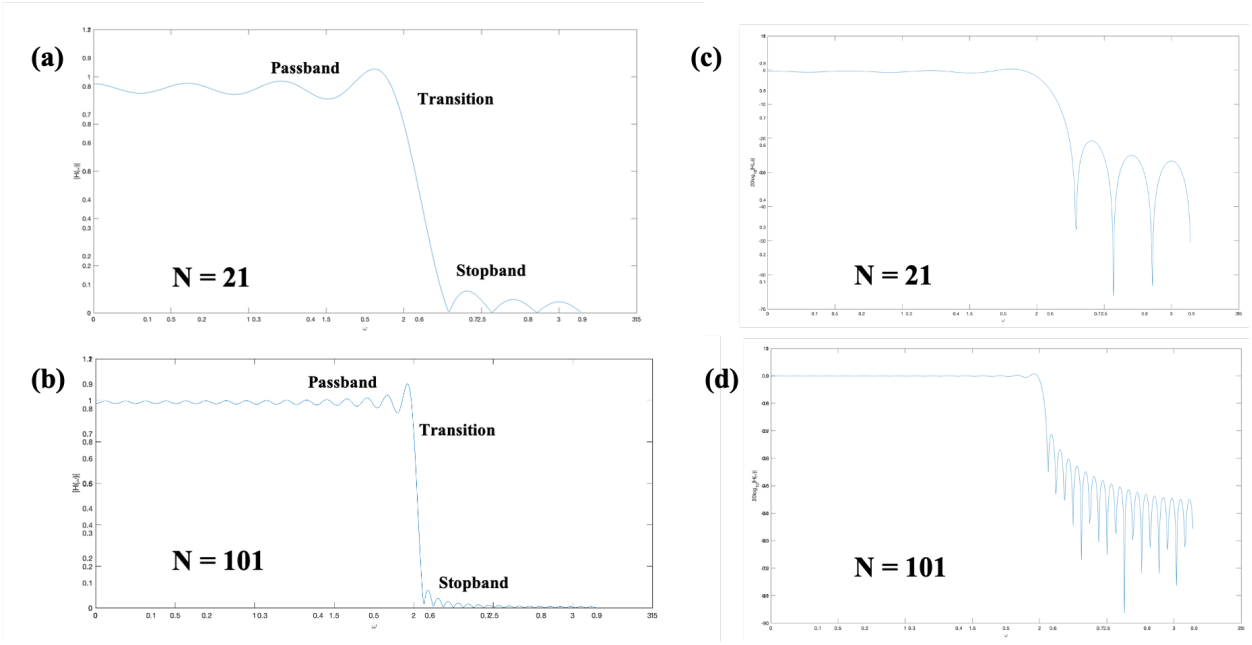

Figure 1: Effects of truncation on an ideal low-pass filter (ILPF). (a) Truncated ILPF in linear scale with $N = 21$ ($M = 10$), indicating the passband, transition, and stopband regions. (b) Truncated ILPF in linear scale with $N = 101$ ($M = 50$), indicating the passband, transition, and stopband regions. (c) Truncated ILPF in log scale with $N = 21$. (d) Truncated ILPF in log scale with $N = 101$.

1.2 Optimal Order Filter Design

Here we design a symmetric, low-pass FIR filter using the parameters $\omega_p = 1.8, \omega_s = 2.2, \delta_p = 0.05, \delta_s = 0.005$. Using an optimal order filter algorithm with a sampling rate just above the Nyquist rate ($f_s = 5.5$ [normalized freq.]), we get that the minimum order filter has order $N = 22$ with a measured stopband gain of $\delta_s = 0.0047$ and passband gain of $\delta_p = 0.0107$ dB. The resulting FIR filter is shown in Figure 2(a). However, the filter order can be adjusted to meet our constraints on the stopband/passpand gains and frequencies. Hence, we were able to achieve a passband gain of $\delta_p = 0.0236$ and stopband gain of $\delta_s = 0.0025$ by increasing N to 29. This result is plotted in Figure 2(b). Hence by increasing the filter order, a marginal improvement in meeting our specifications. However, the optimal order filter was still able to get very close to our specified constraints ($|\delta_s - \delta_s^{opt}| = 0.0003$ and $|\delta_p - \delta_p^{opt}| = 0.04$).

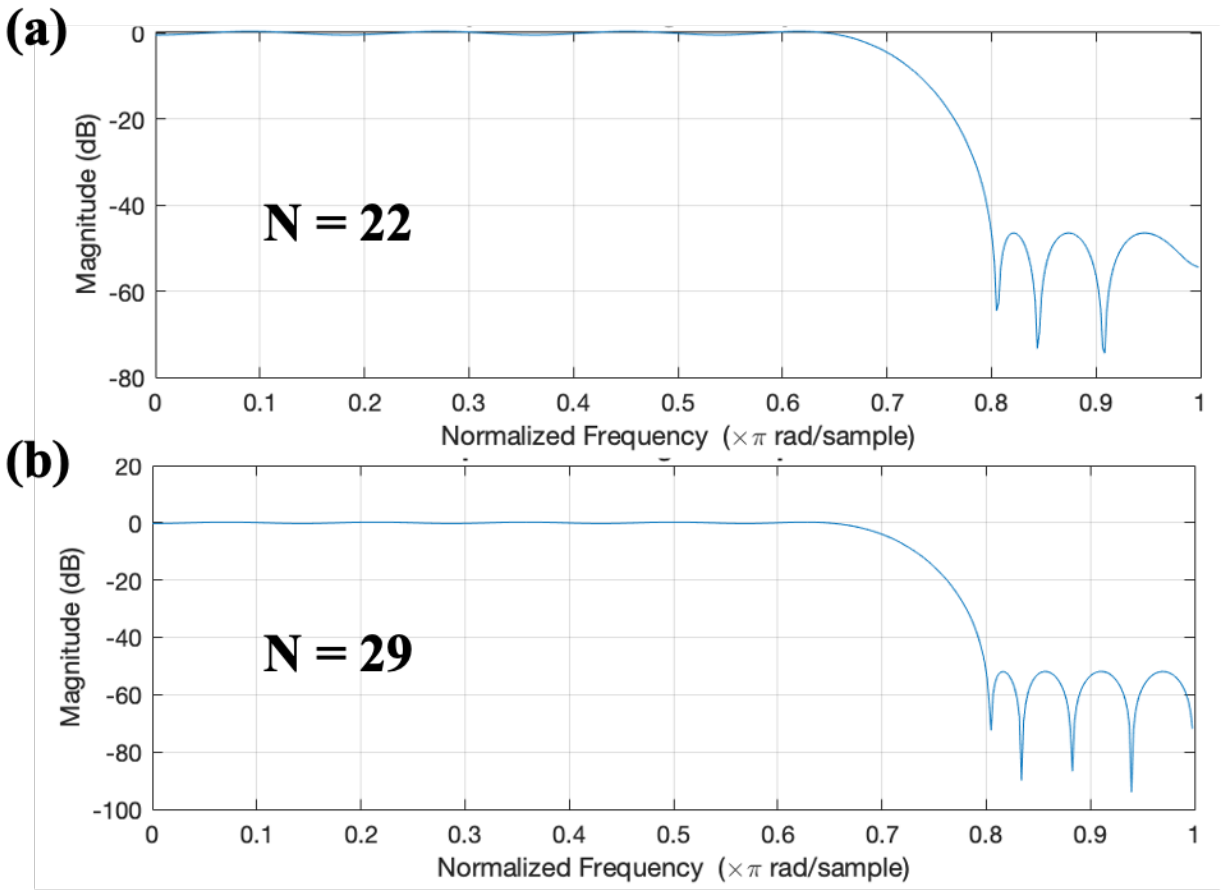

Figure 2: Optimal order filter design. (a) Filter frequency response magnitude of size $N = 22$ obtained with optimal order design (plotted over normalized frequency). (b) Filter frequency response magnitude of size $N = 20$ obtained with heuristic design (plotted over normalized frequency).

1.3 Optimal Filter Design among different Filter Types

Here we design a filter for the removal of high pass noise in a speech signal. We take the ripple magnitude to be δ and the expressions for minimum and maximum passband gain ($G_{pb,min}, G_{pb,max}$) and maximum stopband gain ($G_{sb,max}$) are given in Eqt. 3. (with η as the stopband gain).

$$\begin{aligned} G_{pb,min} &= 20(\log_{10}(1-\delta)+k) \\ G_{pb,max} &= 20(\log_{10}(1+\delta)+k) \\ G_{sb,max} &= 20(\log_{10}\eta+k) \end{aligned} \tag{3}$$

From this, we can solve for k to get,

$$G_{pb,max} - G_{pb,min} = 20\log\frac{1+\delta}{1-\delta}$$

$$k = \frac{G_{pb,max}}{20} - \log_{10}(1+\delta)$$

$$\eta = 10^{G_{sb,max}/20-k}$$

Where we can solve δ, k, η with some iterative approach as these solutions have no closed form solution. Here, we take $G_{pb,max} = 40$ dB, $G_{pb,min} = 37$ dB, and $G_{sb,max} = -55$ dB. We find that the parameters meeting our constraints are $\delta = 0.171, k = 1.931, \eta = 2.08 \times 10^{-5}$. Using these parameters, we can now construct a series of low-pass filters that can be implemented on our signal. Specifically, we consider Butterworth, Chebyshev I, and Chebyshev II filters with a passband edge of $\omega_p = 2500$ Hz and stopband edge of $\omega_s = 4000$ Hz.
Using our constraints on the gain of the system ($G_{pb,max} = 40$ dB, $G_{pb,min} = 37$ dB, and $G_{sb,max} = -55$ dB), we find optimal order filter designs for the Butterworth, Chebyshev Type I, and Chebyshev Type II filters. Using the optimizer, we find minimum orders of $N = 4, 3, 3$ for the Butterworth, Chebyshev Type I, and Chebyshev Type II filters. From this, we can get the number of multiplications per sample for an input signal of size M. This will be $8M, 6M, 6M$ for the each of the three filters. Plotted in Figures 3, 4, and are the FIR frequency responses in log scale (a), frequency responses linear scale (b), and group delays (c) for the Butterworth, Chebyshev I, and Chebyshev II optimal filters. Plotted in Figures 6-8 (a)/(b) are the impulse responses and pole-zero plots for the three filters. We finally applied each filter to a noisy audio signal. Listening to the original signal, the noise is seen in the high frequency regime. Hence, applying the Butterworth filter cuts out most of this noise and it appears as if there is no sound with the filter applied. The same effect is heard with the Chebyshev I filter, but instead there is an initial burst of sound. However, the later parts of the signal show no sound. The Chebyshev II filter revealed he noisiest response. Most of the high frequency components were cutoff, however some middle frequency components remained. It appears as if the the noise amplitude was suppressed but not entirely cut out.

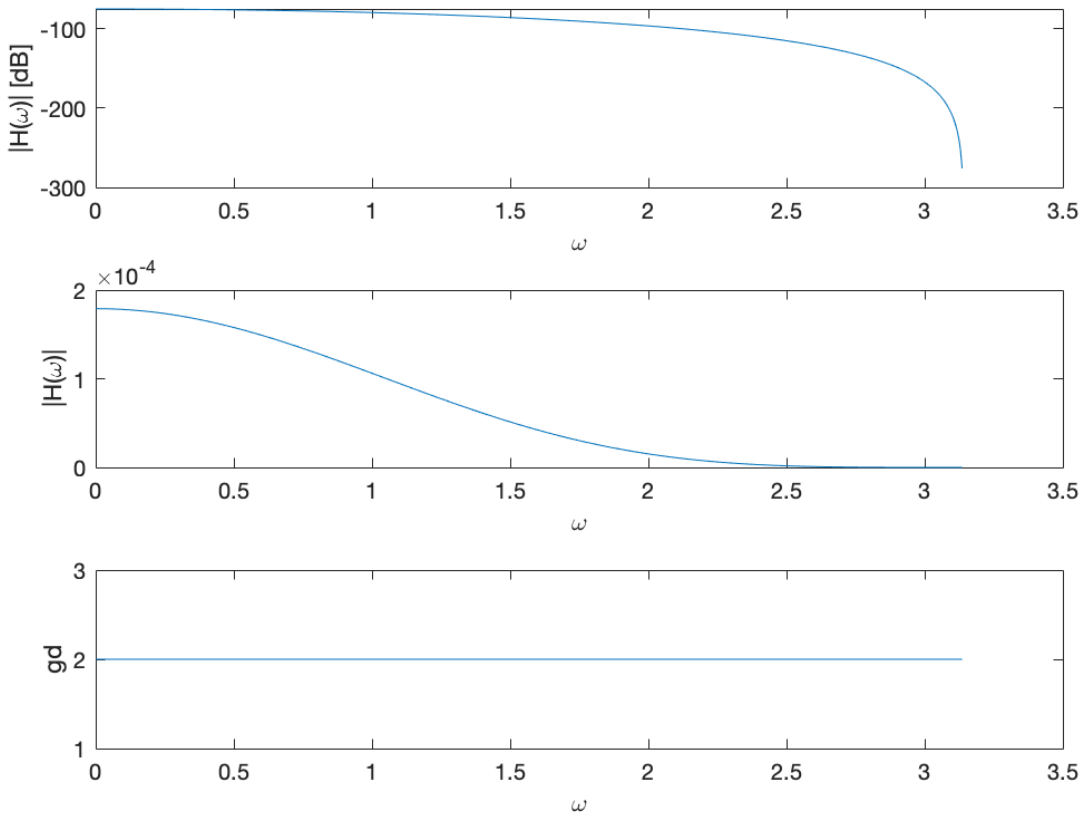

Figure 3: Optimal Butterworth Filter. (a) Magnitude of filter's frequency response in log-scale [top], (b) Magnitude of filter's frequency response in linear scale [middle], (c) group delay of filter [bottom].

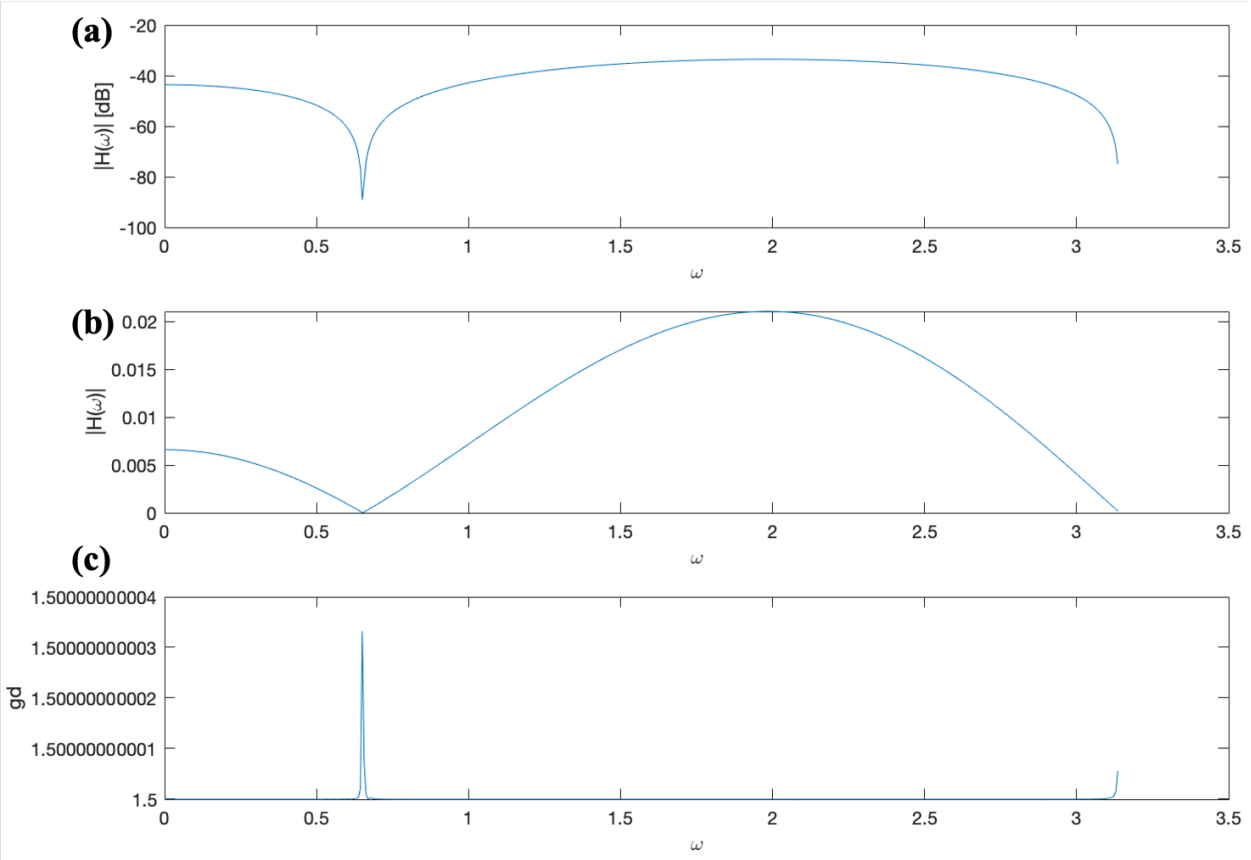

Figure 4: Optimal Chebyshev I Filter. (a) Magnitude of filter's frequency response in log-scale [top], (b) Magnitude of filter's frequency response in linear scale [middle], (c) group delay of filter [bottom].

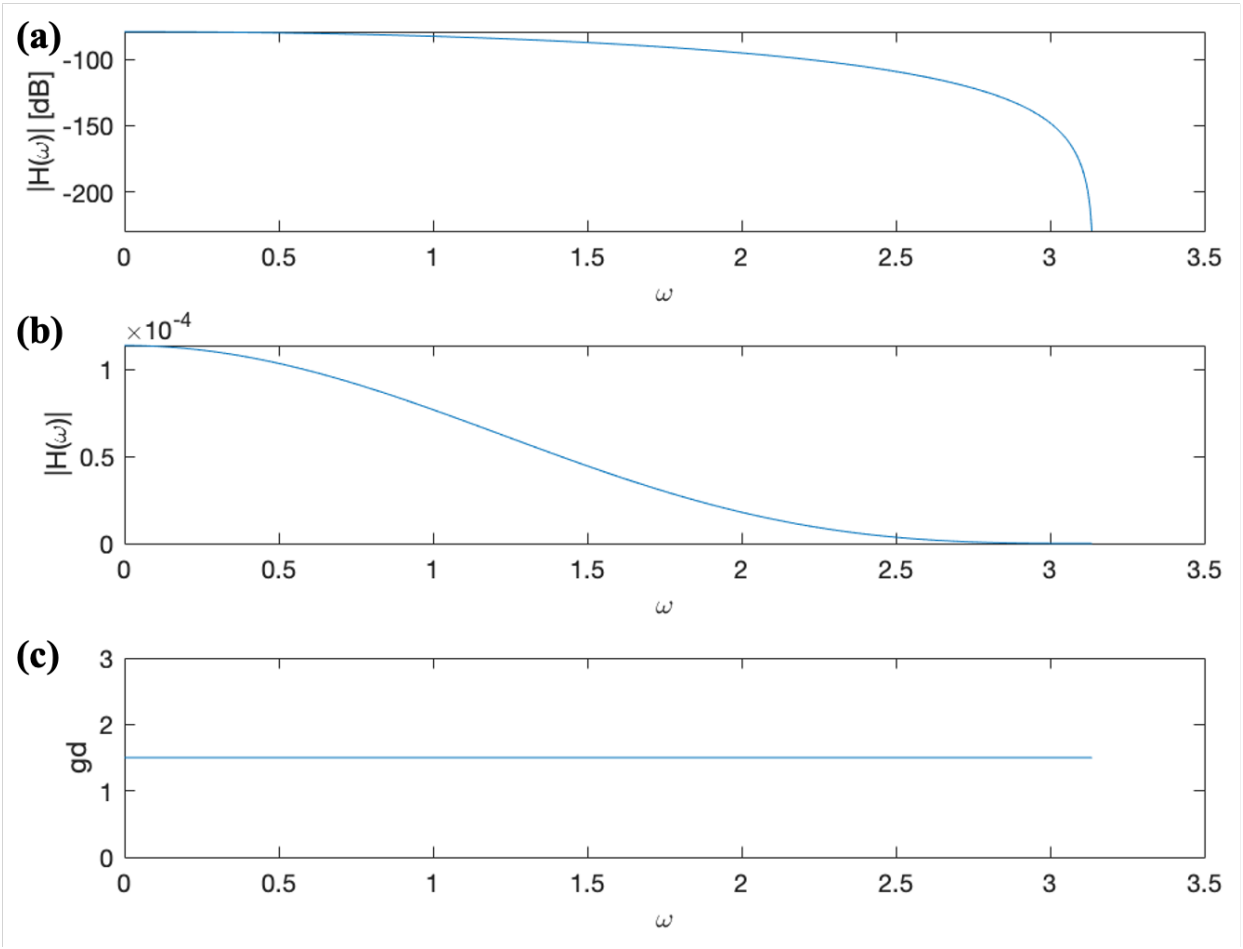

Figure 5: Optimal Chebyshev II Filter. (a) Magnitude of filter's frequency response in log-scale [top], (b) Magnitude of filter's frequency response in linear scale [middle], (c) group delay of filter [bottom].

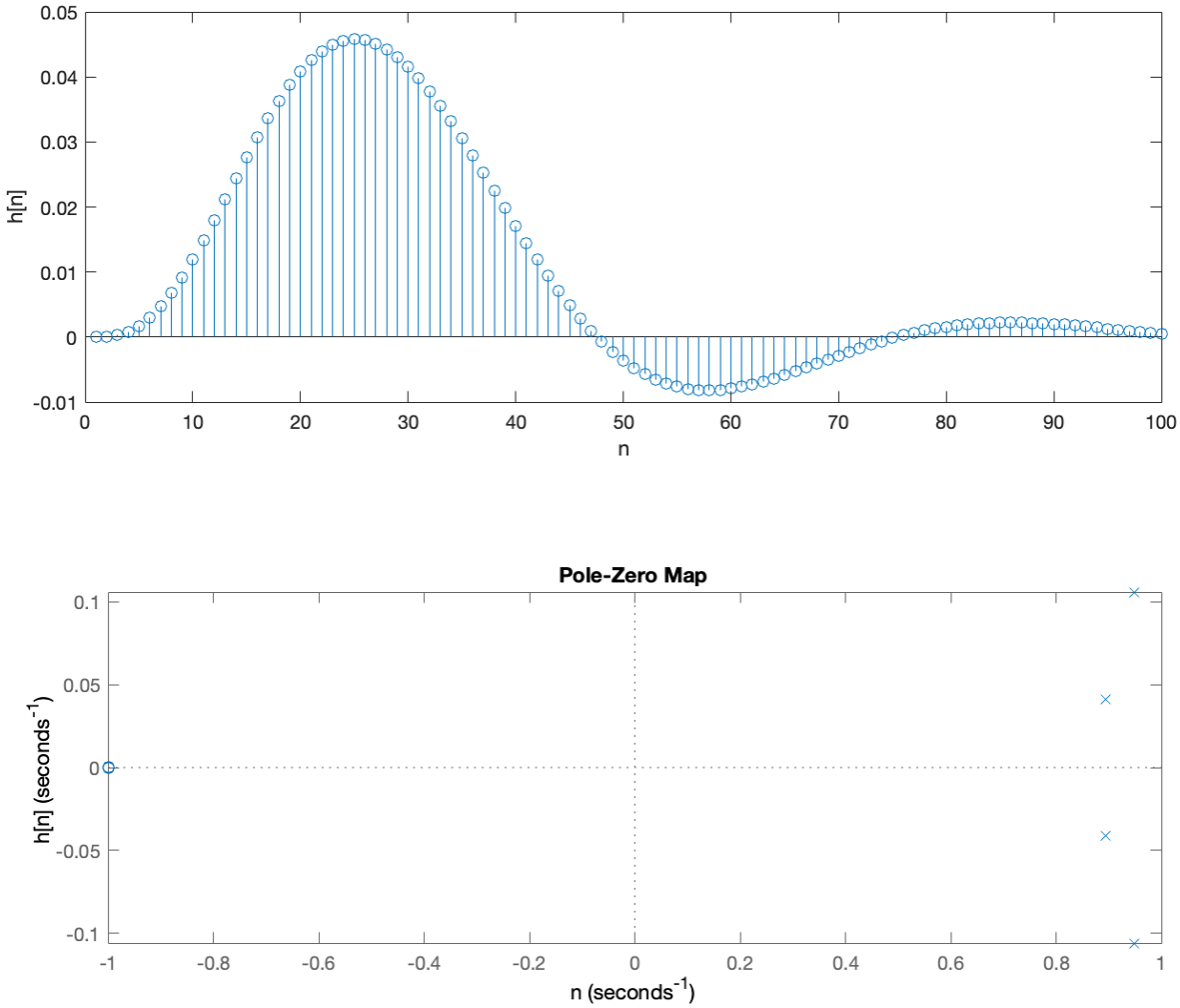

Figure 6: Butterworth Filter Impulse and Pole-Zero. (a) Impulse response $h[n]$ (b) Pole-Zero diagram.

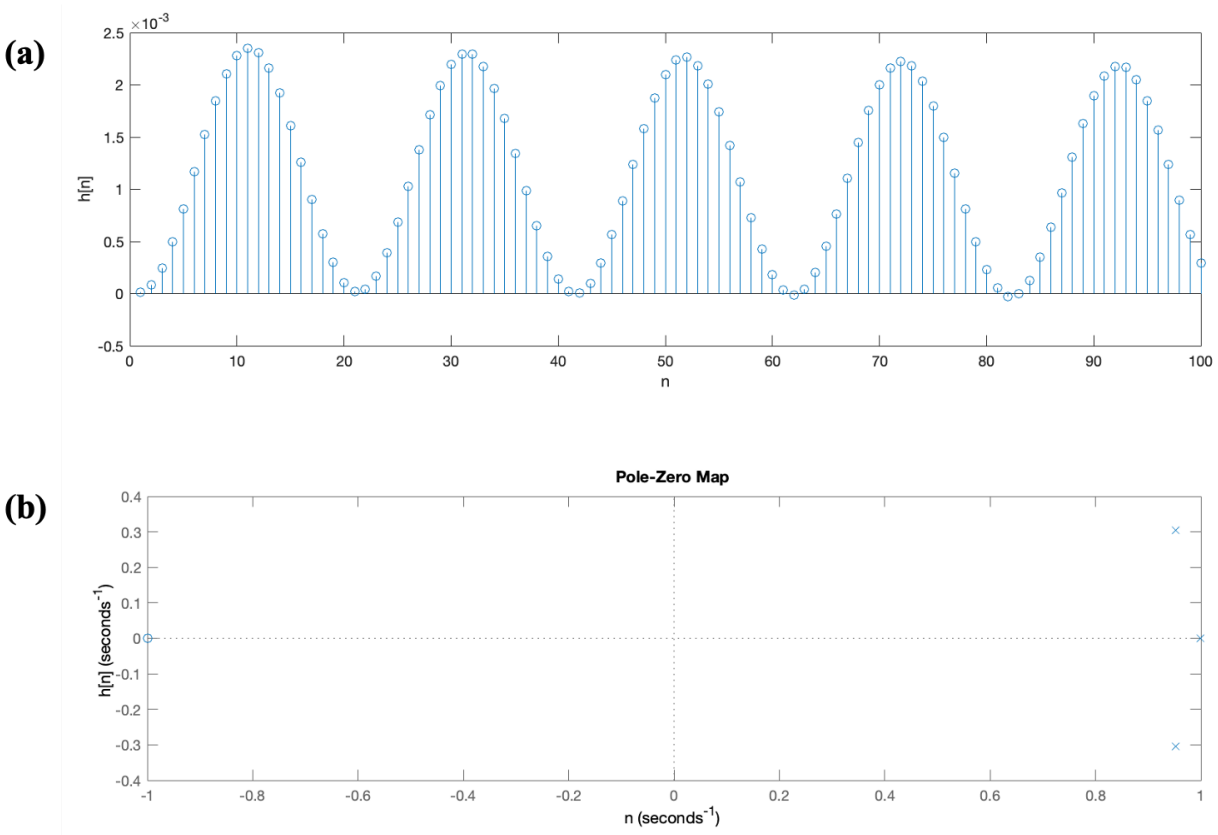

Figure 7: Chebyshev Type I Filter Impulse and Pole-Zero. (a) Impulse response $h[n]$ (b) Pole-Zero diagram.

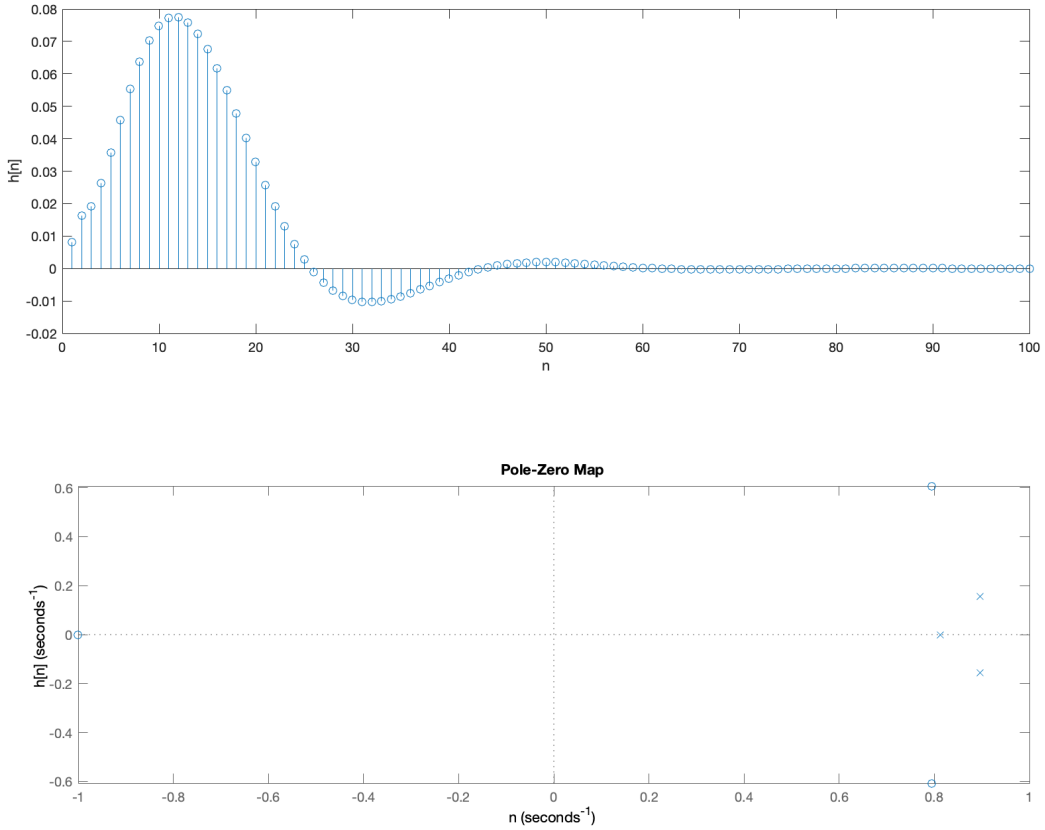

Figure 8: Chebyshev Type II Filter Impulse and Pole-Zero. (a) Impulse response $h[n]$ (b) Pole-Zero diagram.

2 Multi-Channel Filter Banks

2.1 Design of a 4-channel octave band scheme

Construction of Filter bank: Here we design a 4 channel octave band scheme. In particular, we construct a filter bank by decomposing a full frequency band ($[0, \pi]$) into 4 subbands. These filters comprise a low-pass filter in the range of $[0, \pi/8]$, a band-pass filter from $(\pi/8, \pi/4]$, another band-pass filter from $(\pi/4, \pi/2]$, and a high-pass filter from $(\pi/2, \pi]$. Truncated versions of these filters were constructed to form a filter bank and the corresponding frequency response in both linear and log-scale are plotted in Figure 9(a)/(b).

Testing Filter bank:
Each band of the filter bank is then applied to a test signal given by the expression Eqt. (4).

$$x_{test}[n] = \sin(0.3n) + \sin(0.55n) + \sin(1.3n) + \sin(2.0n), 1 \leq n \leq 1,000 \tag{4}$$

Both the impulse and frequency response of this test input is shown in Figure 10 (a)/(b). This test signal has normalized frequency components $\omega = 0.3, 0.55, 1.3, 2.0$, each corresponding

to a frequency band in our filter design. Hence, we would expect that after convolving the impulse response of the filter with x_{test}, only the frequency components corresponding each band of the filter bank should remain. Now applying each band of the filter bank to $x_{test}[n]$, we obtain both the impulse and frequency response which are plotted in Figure 11. Figure 11 (a)-(d) shows the impulse response of the output for each band of the filter bank. It is more insightful to look at the frequency response for each, shown in Figure 11 (e)-(h). Here, we can clearly see that the filter bank is effective in selecting all the frequencies for the lowest three bands as the resulting frequency responses are delta functions. However, the frequency response for the highest band output has multiple frequency components but with a max amplitude around $\omega = 2.0$.

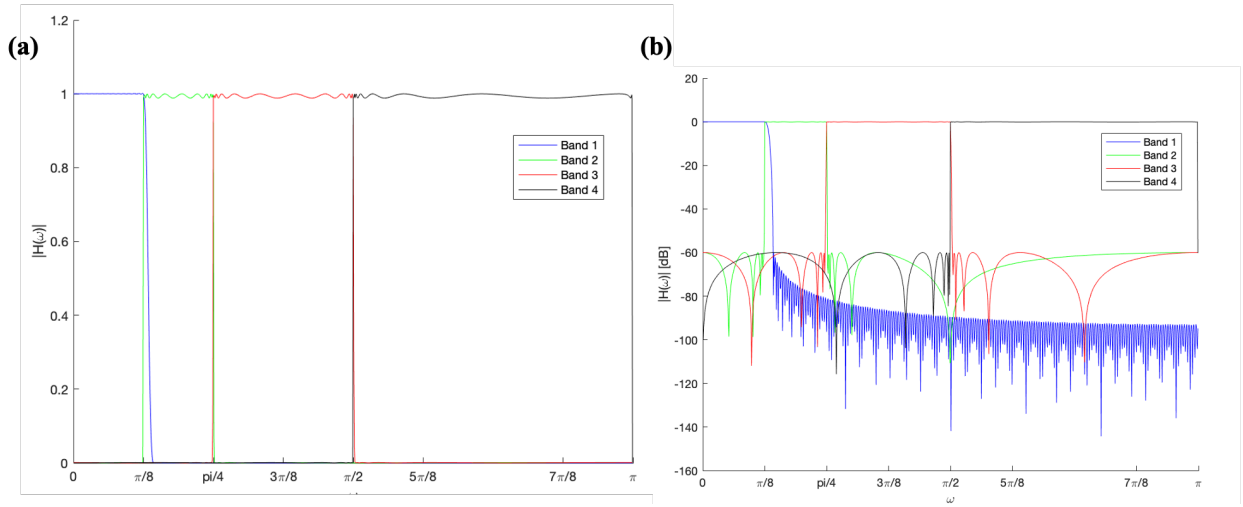

Figure 9: Filter bank design: (a) Magnitude of frequency response of 4-channel octave filter bank in linear scale, (b) Magnitude of frequency response of 4-channel octave filter bank in log-scale.

$x_{test}[n]$ has 4 frequency components $\omega = 0.3, 0.55, 1.3, 2.0$ each within one of the four bands of the filter bank we designed.

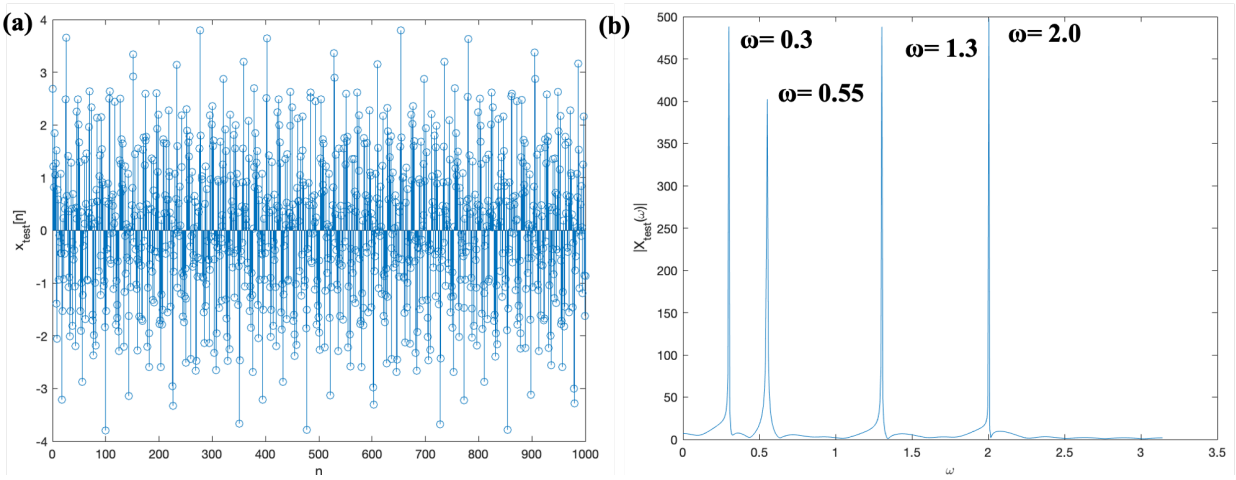

Figure 10: Test input signal. (a) Impulse response of $x_{test}[n]$, (b) frequency response of test signal $|X_{test}(\omega)|$.

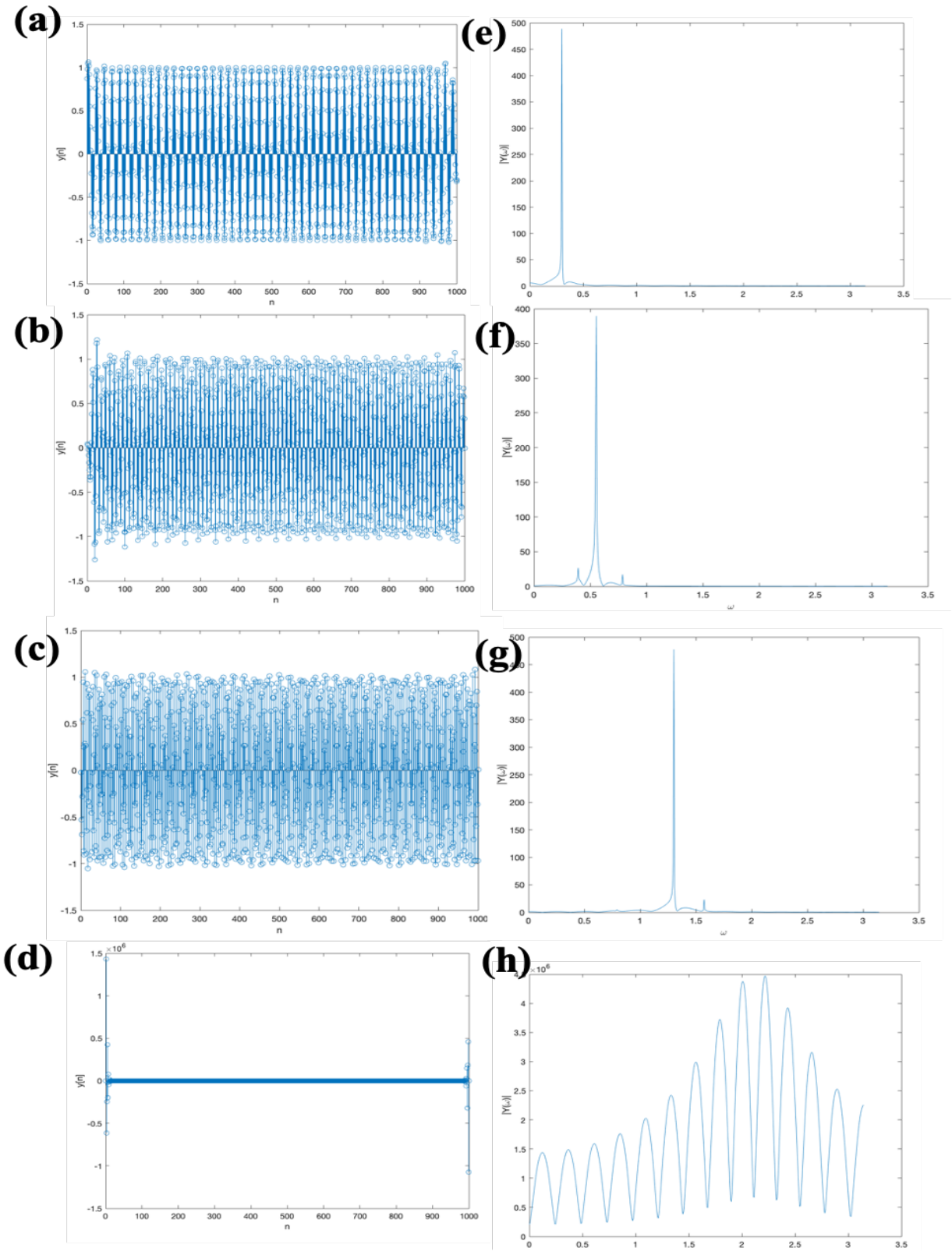

Figure 11: Filter bank applied to test input signal. (a) Impulse response of first band applied to x_{test}, (b) Impulse response of second band applied to x_{test} , (c) Impulse response of third band applied to x_{test} , (d) Impulse response of fourth band applied to x_{test}, (e) Frequency response of first band applied to X_{test}, (f) Frequency response of second band applied to X_{test} , (g) Frequency response of third band applied to X_{test} , (h) Frequency response of fourth band applied to X_{test}.

3 Filter Banks on Audio Signals

Here, we implement our filter bank from the previous section on an audio signal. In particular, we use the filter bank to boost the bass and high-frequency components of the signal. Hence, we use the first and fourth bands from the filter bank to do this. The original audio signal in the frequency domain is shown in Figure 12(a). Applying the bass boost (applying first filter and then amplify) yields frequency response in (b). Applying the high-frequency boost gives the resulting frequency response in Figure 12(c).

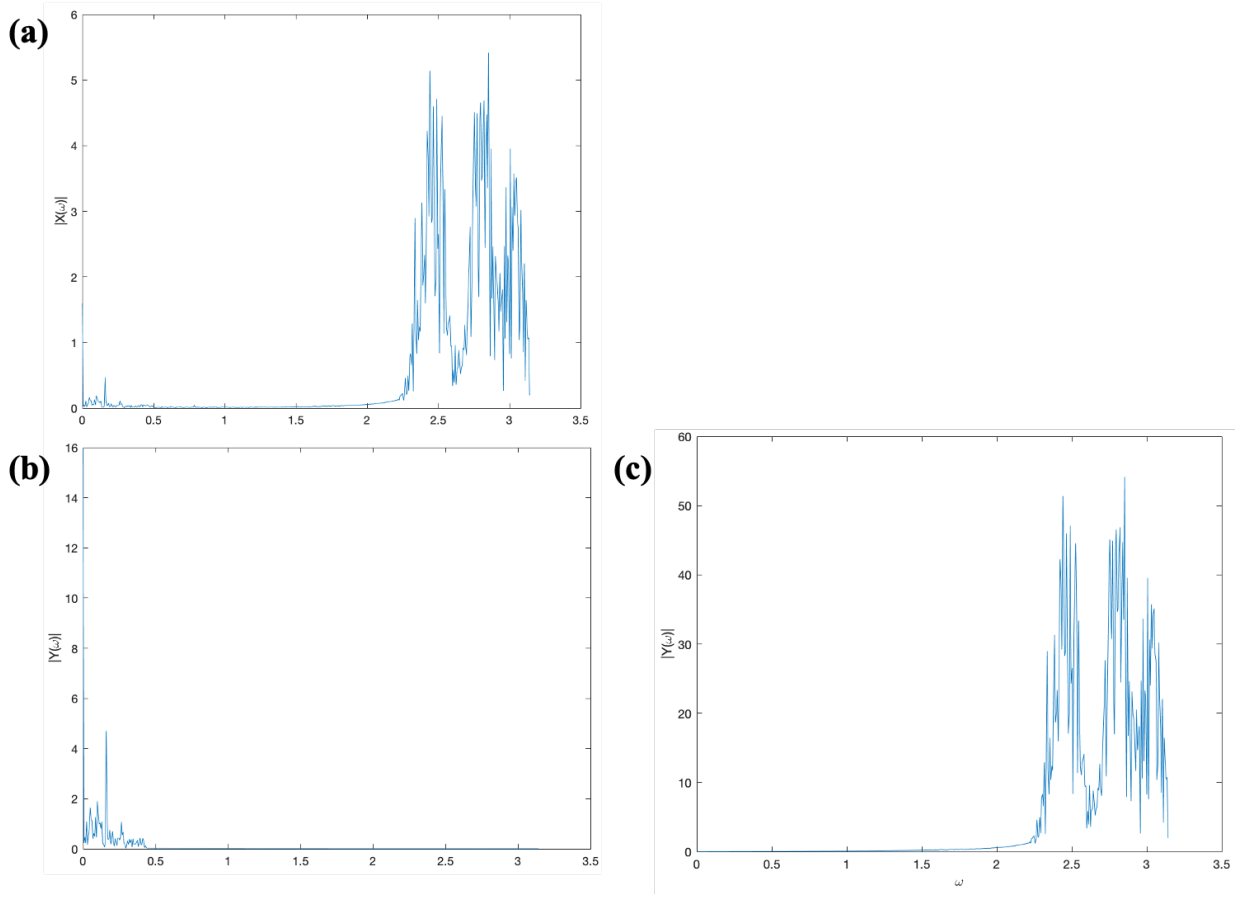

Figure 12: Effect of filter bank on bass and treble boost of audio signal: (a) Magnitude of the original audio signal in the frequency domain, (b) magnitude frequency response of bass-boosted audio signal, (c) magnitude frequency response of treble-boosted audio signal.

4 Filter Banks on Images

Here we use a 2-channel PR-FB to filter a 2D image of an owl. We use a filter order of 7. The filter bank comprises 2 analysis filters (H_0 and H_1) and 2 synthesis filters (G_0 and G_1). The filters used, in addition to the effect of each filter is plotted in Figures 13.

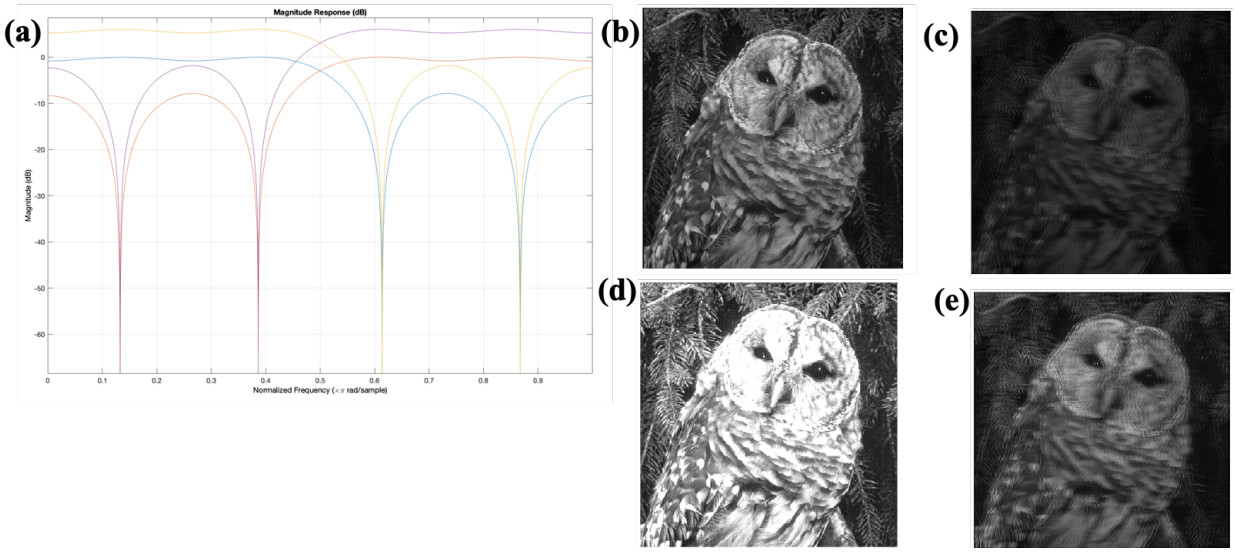

Figure 13: 2-channel PR-FB applied to 2D image. (a) Analysis and synthesis high pass and low pass filters in the frequency domain, (b) H_0 applied to image, (c) H_1 applied to image, (d) G_0 applied to image, (e) G_1 applied to image.

Appendix: Attached Code

Truncate script.

```
function [n, h] = LPFtrunc(N)
    w_c = 2.0;
    M = floor(N/2);
    n = linspace(-M,M,2*M);
    h = (w_c/pi)*sinc(w_c*n/pi);
end
```